Review of Scientific Instruments

A new approach of electrochemical etching fabrication based on drop-off-delay control

Cite as: Rev. Sci. Instrum. **90**, 074902 (2019); https://doi.org/10.1063/1.5094470
Submitted: 02 March 2019 . Accepted: 27 June 2019 . Published Online: 17 July 2019

Sheng Yang, Weinan He, Can Li, Yuexia Han, and Ning Gu


View Online

Export Citation

CrossMark

ARTICLES YOU MAY BE INTERESTED IN

Spatially resolved solid-phase temperature characterization in a sillimanite tube furnace using a broadband two-color ratio pyrometry
Review of Scientific Instruments **90**, 074903 (2019); https://doi.org/10.1063/1.5088149

Servo X-Y biaxial feed system of flux switching permanent magnet linear motor
Review of Scientific Instruments **90**, 074703 (2019); https://doi.org/10.1063/1.5065451

Angle-resolved broadband ferromagnetic resonance apparatus enabled through a spring-loaded sample mounting manipulator
Review of Scientific Instruments **90**, 076103 (2019); https://doi.org/10.1063/1.5113773

© 2019 Author(s).

Review of Scientific Instruments ARTICLE scitation.org/journal/rsi

A new approach of electrochemical etching fabrication based on drop-off-delay control

Cite as: Rev. Sci. Instrum. 90, 074902 (2019); doi: 10.1063/1.5094470
Submitted: 2 March 2019 • Accepted: 27 June 2019 •
Published Online: 17 July 2019

View Online Export Citation CrossMark

Sheng Yang, Weinan He, Can Li, Yuexia Han, and Ning Gu[a)]

AFFILIATIONS

Jiangsu Key Laboratory for Biomaterials and Devices, School of Biological Sciences and Medical Engineering, Southeast University, Nanjing 210009, China

[a)]**Author to whom correspondence should be addressed:** guning@seu.edu.cn. **Tel.:** +86-25-83794960.

ABSTRACT

W-Pt micro-nano-thermocouple is a brand new sensor for intracellular temperature measurement. As a nanodevice, it is based on the electrochemical etching method of which the shape is directly related to the performance. Although much research has been done on how to control the shape of the tungsten tip through electrochemical etching method, preparing different shapes requires different fabrication methods. In this article, we proposed a flexible and general control method which can fit all the fabrication methods by merely modifying the software. Moreover, this method based on drop-off-delay time control is capable of controlling the duration of the electrochemical reaction during the final formation of the tungsten tip. Based on this method, the cone angle can be set to any value from 5° to 30° with the radius of curvature maintaining from 2 nm to 5 nm. Additionally, the sophisticated fabrication of W-Pt micro-nano-thermocouple was designed to be automatically completed by three workshops in batches. The efficiency and uniformity of W-Pt micro-nano-thermocouple fabrication were well improved.

Published under license by AIP Publishing. https://doi.org/10.1063/1.5094470

I. INTRODUCTION

Temperature is one of the most significant biological indexes in organisms. For decades, there has been extensive study on intracellular temperature measurement at the single-cell level for meaningful biological information. A quantity of methods have been proposed,[1,2] but most of them are based on the imaging analysis. Limited by the process time, the imaging method always has a long response time (more than 10 μs) or even cannot carry out real-time measurement. Wang *et al.* have designed a sandwich-structure thermocouple,[3] which consists of a tungsten substrate, insulating layer and platinum film, in micro-nano-scale (W-Pt micro-nano-thermocouple). The W-Pt micro-nano-thermocouple (W-Pt TC) has a long response time of 400 ns, and the resolution can be very high when the appropriate backend circuit is used. The W-Pt TC uses tungsten as its substrate, which means that the final profile of thermocouple is determined by the tungsten tip. The electrochemical etching,[4] proposed by Ibe *et al.*, is widely used in the fabrication of the ultra-sharp tungsten tip for its stability, reproducibility, and controllability.[5,6] The profile of the tungsten tip can be controlled by several etching parameters: etching voltage, tension, meniscus, and solution. Most of the researchers focus on the etching voltage control, such as "drop-off" time reduction,[7,8] multistep etching with different voltages.[7,9–11] Tension is difficult to control, and the yield rate will also be affected.[12,13] Recently, researchers have become increasingly interested in meniscus control. This method is implemented by the movement of the tungsten tip during the electrochemical etching procedure. Slowly lifting up the tungsten tip[6,14] and oscillating the tungsten tip[7] make the shape different compared with the static method during the electrochemical etching procedure. The study of methods controlling more than one parameter simultaneously also attracts more and more attention in recent years.[14,15]

The W-Pt TC can be applied in the biological experiment with high reliability and convenience. However, the fabrication of W-Pt TC designed by Wang *et al.* is very sophisticated. The tungsten substrate is prepared by the electrochemical method, and the insulating layer must be implemented by the micro-nano-manipulator operated by the experimenter. Meanwhile, W-Pt TC cannot be reused in measurement to prevent the cross-infection. In this condition, the research on batch fabrication is necessary for the sake of reducing the dependence of the experimenter's skills and experience.

Furthermore, W-Pt TC with different profiles and shapes will affect the use and the performance. Although a considerable amount of research has been devoted to thin-film thermocouple and the size effect of thin-film, less attention has been given to three-dimensional heterojunction and its size effect in nanoscale. It remains unclear whether heterojunction with different three-dimensional profiles or shapes has a relationship with the W-Pt TC's Seebeck coefficient or other performance. As discussed above, the profile and the shape of W-Pt TC are determined by the tungsten substrate. However, different researchers choose different strategies to control the final profiles with different control circuits. It is meaningful to design a flexible and general control circuit for those who want to fabricate tungsten tips, or W-Pt TC, with different profiles. Moreover, we noticed that most researchers focus on reducing the drop-off time with high-speed devices or sophisticated circuit, while there are few attempts to control the drop-off-delay time. It would be significant to investigate the relationship between drop-off-delay time and profiles.

This paper introduces a technique of batch and automatic fabrication of W-Pt TC. Moreover, a general control circuit with controllable drop-off-delay time for the electrochemical etching method has been developed, and it is shown to be stable and reproducible in the experiment. With this new technique, W-Pt TC can be fabricated without a heavy reliance on the operator's experience. Different profiles, such as an angle of cone and different appearance, can be fabricated through modification in the software, while hardware configuration remains unchanged.

II. METHODOLOGY

As is shown in Fig. 1 **Perspective**, the W-Pt TC is composed of three different materials: tungsten, polyurethane, and platinum. The structure of sandwich aims to miniaturize the sensor. The fabrication process can be divided into three steps, as shown in Fig. 1. The reason we focused on are Step1 and Step2, is that, the last step is completed by the ion sputtering coater (Quorum Q150TS). At this point, the etch workshop [Fig. 2(d)], corresponding to Step1, and the wrap workshop [Fig. 2(b)], corresponding to Step2, can be

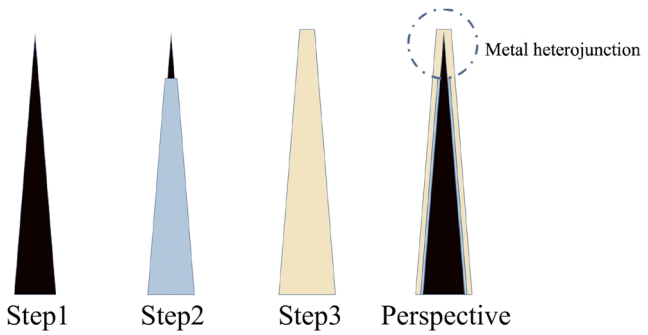

FIG. 1. Schematic views of fabrication W-Pt TC step by step. **Step1**: To prepare tungsten substrate using electrochemical etching. **Step2**: To attach insulating layer, which is made of polyurethane, to the tungsten substrate. **Step3**: To coat platinum film on the tungsten substrate processed by Step2. **Perspective**: The perspective of the W-Pt TC.

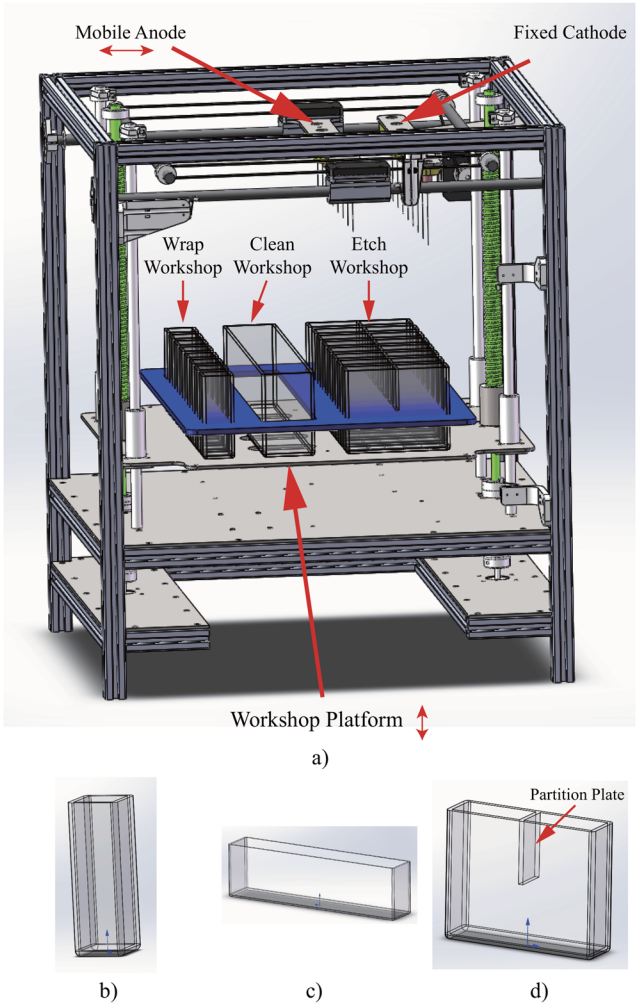

FIG. 2. Schematic views of apparatus for W-Pt TC fabrication. (a) W-Pt TC Fabrication Platform. (b) Wrap workshop's container. (c) Clean workshop's container. (d) Etch workshop's container.

added to the automation process. Moreover, a clean workshop is also necessary to be added between the etch workshop and wrap workshop. The underlying rationale for this will be explicated in Sec. II B. Figure 2 presents the structure of the apparatus. It consists of the workshop platform, which can move in the vertical direction, and the mobile anode, which can move in the horizontal direction. The mobile anode carries the tungsten from one workshop to another while the workshop platform can carry out the task. Each workshop can fabricate eight W-Pt TC in parallel.

A. Etch workshop

Electrochemical etching has been widely used in fabricating tungsten tips. The conventional method is that researchers would insert a thin tungsten bar into the sodium hydroxide solution [depicted in Fig. 3(a)]. Equation (1) shows the electrochemical

Published under license by AIP Publishing

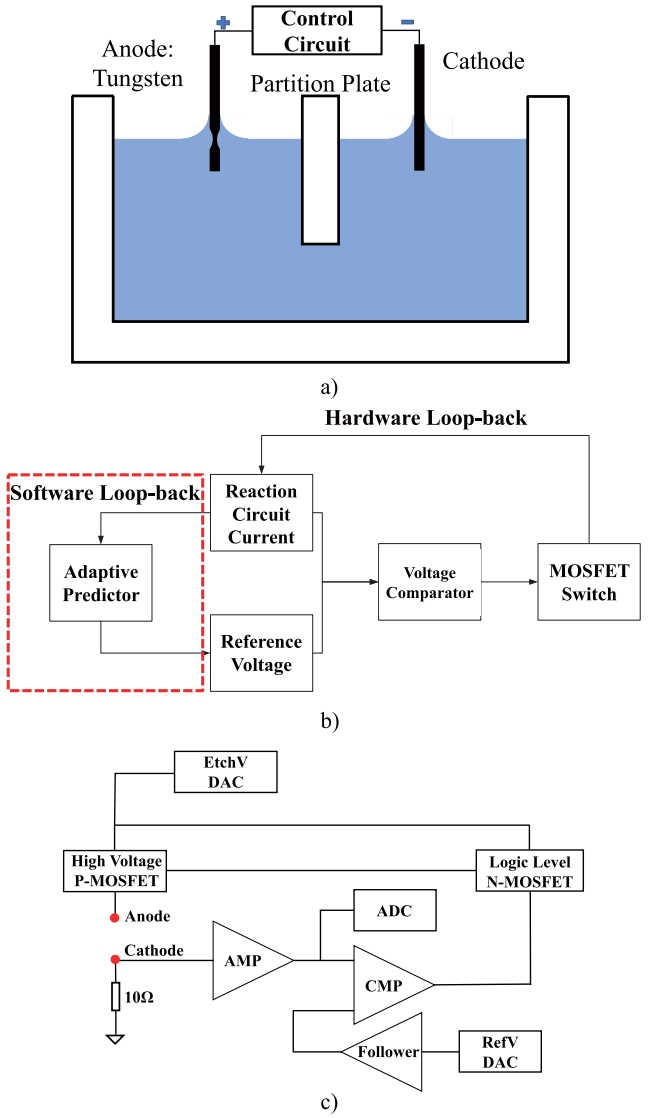

FIG. 3. The schematic diagram of electrochemical etching for fabrication tungsten tip. (a) shows the basic configuration of the electrochemical reaction. (b) excluding content in the red frame is the diagram of classic method's "control circuit" depicted in (a). (b) including content in the red frame and (c) is the method proposed in the article. The adaptive predictor in (b) is the combination of "ADC" and "Ref DAC" shown in (c). In addition, "AMP" represents "Voltage Amplifier," "CMP" represents "Voltage Comparator," "Follower" represents "Voltage Follower," "ADC" represents "Analog-to-Digital Converter," and "DAC" represents "Digital-to-Analog Converter."

reaction taking place inside the system,

$$\begin{aligned} &Anode: W + 8\,OH^- \longrightarrow WO_4^{2-} + 4\,H_2O + 6\,e^-, \\ &Cathode: 6\,H_2O + 6\,e^- \longrightarrow 3\,H_2 + 6\,OH^-, \\ &Full: W + 2\,OH^- + 2\,H_2O \longrightarrow WO_4^{2-} + 3H_2. \end{aligned} \tag{1}$$

Anode's electrochemical reaction will take place at the liquid gas interface. A meniscus, which leads to the formation of the tip in the tungsten bar's neck as shown in Fig. 3(a), will form in the interface due to the tension of sodium hydroxide solution. Figure 4(a) exhibits the electrochemical reaction's signal (red one) captured by NI MyDAQ with 10 kSPS (SPS, Sample Per Second). It can be seen clearly that a "drop-off," which accompanies the formation of the tip, occurs in the red signal in Fig. 4(a). As exhibited in Fig. 3(b) excluding the part in red frame, in the classic method, the control circuit with the single hardware feedback loop is used to detect this "drop-off" and cuts off the etching power source immediately to prevent the continuous current from destroying the tip. The reason

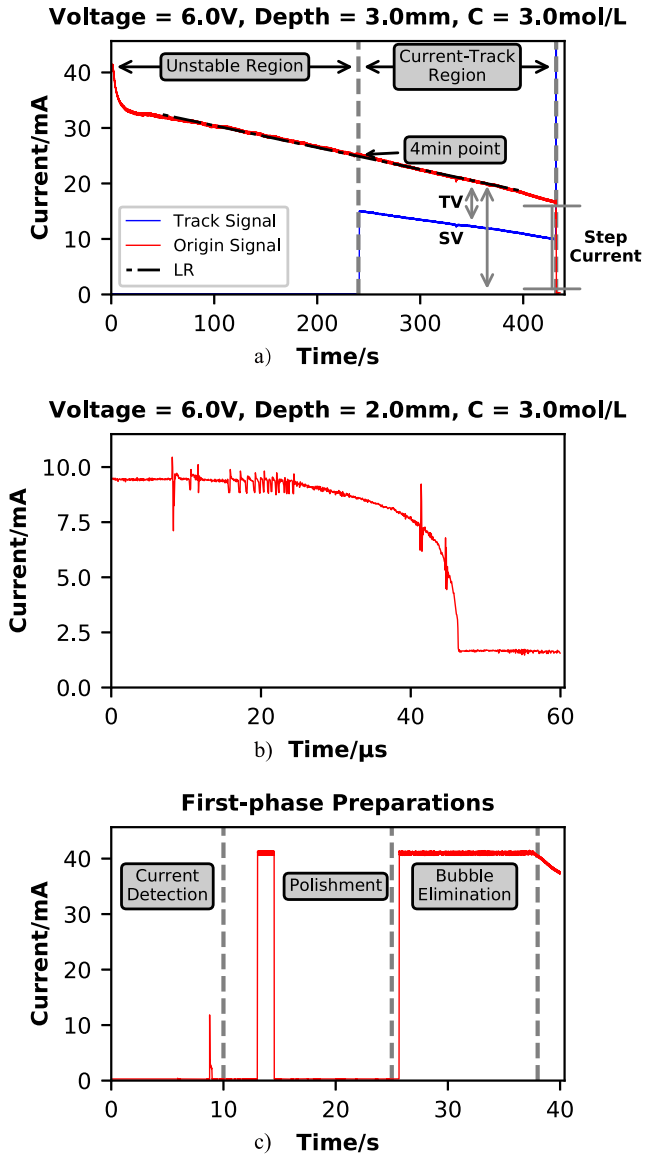

FIG. 4. Using data acquisition card with different sample rates to collect data. (a) and (c) were acquired with 10 kSPS, and (b) was acquired with 20MSPS. (a) shows voltages of voltage comparator's two inputs. (b) is snapshot of "drop-off" with no control. (c) exhibits the preparation procedure before electrochemical etching's start.

Published under license by AIP Publishing

for using hardware feedback loop rather than software control is that the response time for "drop-off" is limited to a small range (less than 20 μs, which is the drop-off time t_d). As is shown in Fig. 4(b), a data acquisition card with 20MSPS was utilized to observe the "drop-off" period. Although many studies has been done, most of them only focus on reducing the "drop-off" time, which cannot break away from the traditional structure [Fig. 3(b) excluding the part in red frame]. This "drop-off" period is directly related to the formation of the tungsten tip. During this period, both the electrochemical action and the tension played a role in the formation of the final shape. Therefore, the electrochemical action's lasting time on the formation of the tip can be under control if the delay time after the "drop-off" starts (drop-off-delay time) can be controlled. In other words, the technique needs to be developed to stop the electrochemical reaction at any point of time during the "drop-off" period.

The straightforward scheme is using a high-speed processor, an A/D (Analog-to-Digital) convertor, and a D/A (Digital-to-Analog) convertor. In fact, some researchers have used this scheme with the DSP (Digital Signal Processing) chip controlled circuit, but they have paid scant attention to control the drop-off period. Nevertheless, this scheme is difficult to implement. According to nyquist sampling theorem, the relationship among drop-off time t_d, drop-off control's time resolution t_r, and A/D convertor's sample rate f_{sps} can be established as

$$f_{sps} \geq \frac{5}{t_r} \quad (t_r < t_d). \tag{2}$$

If a higher drop-off control time resolution is required, the sample rate will also need to be higher, which may be highly challenging to accomplish. Moreover, this drop-off is not linear during the latter period which requires extra higher sample rate to control the drop-off-delay time. Here, we proposed a scheme which built a relationship between voltage and drop-off control's time resolution t_r. As Fig. 3(b) exhibits, a software feedback loop acting as an adaptive predictor is added to the classic circuit. Figure 3(c) shows the implementation of the scheme. A 10 Ω resister was connected to the cathode to help sample the current signal I_{ece} in the electrochemical etching system. The voltage amplifier (AMP) (AD8009) in Fig. 3(c) was set up as noninverting and $Gain = 10$. Therefore, the AMP's output voltage U_o was $100I_{ece}$. Then, U_o was connected to the voltage comparator's (TLV3501) noninverting input. Meanwhile, U_o was acquired by the microcontroller unit's (MCU's) (STM32F405RGT6) built-in A/D convertor with 1 kSPS. The voltage comparator's inverting input was connected to the MCU's built-in D/A convertor. The voltage comparator's output signal was utilized to control the electrochemical etching's start and stop by a logic level N-MOSFET (CSD16301Q2) and a high voltage P-MOSFET (FDC6302P). The etching voltage, controlled by two MOSFETs, was given by the controllable linear voltage regulator system consisting of a LM350A and a D/A convertor. In summary, the hardware part of the adaptive predictor was composed of an A/D convertor and a D/A convertor connected to the voltage comparator's two inputs. Therefore, the electrochemical etching's current I_{ece} could be obtained, and the reference voltage U_{ref} could be changed in real time. In that, U_o is equal to $100I_{ece}$, where I_{ece} will be replaced with U_o for convenience.

Figure 4(a) illustrates our control strategy which is called current-track. After the electrochemical etching started, the reaction was divided into two regions: unstable region and current-track region. The reason for this division was to avoid the noises and wait for stabilization before the adaptive predictor started. An ideal demarcation point should satisfy the reaction entering stabilization, and electrochemical etching does not stop then. Here, 240 s was chosen as the demarcation point based on the engineering experience. In current-track region, the adaptive predictor started to work. The "drop-off" was supposed to take place within the next 1000 μs after the acquisition point (MCU's built-in A/D convertor's sample rate was set to 1 kSPS). Given that U_o changed slowly (this will be discussed in Sec. III A), the "drop-off" was considered to start from the current acquisition voltage. In other words, the current acquisition voltage was considered as the step voltage, which was labeled SV in Fig. 4(a). The voltage comparator would wait for the voltage of "drop-off" starting [annotated as TV in Fig. 4(a)]. The time parameter was defined r_{track} as

$$r_{track} = \frac{TV}{SV} \approx \frac{t_{delay}}{t_{dropoff}}. \tag{3}$$

Thus, the D/A convertor outputted track signal $V_{da} = (1 - r_{track}) \times SV$ to the reference voltage input pin of the voltage comparator, where SV was the current voltage acquired by the MCU's built-in A/D convertor. Generally speaking, the drop-off-delay time can be controlled by r_{track}.

Another feature of this hardware configuration is current-detection (Fig. 5), which can be used to dip the tungsten bar into the electrolyte with accurate depth. First of all, the D/A convertor outputs 0 V to keep MOSFETs persistently open and the stepper motor moved the tungsten bar down slowly. The A/D convertor sampled the voltage every time the stepper motor moved one step. Moreover, the MCU would record the stepper motor's position when the A/D convertor got the transient signal. Finally, the D/A convertor outputs 5 V to close MOSFETs and lift the tungsten bar up. Using this method, the point where the tungsten bar touches the electrolyte just right can be detected. Hence, it is relatively easy to control the dipping-depth accurately without additional assistance. As Fig. 4(c)

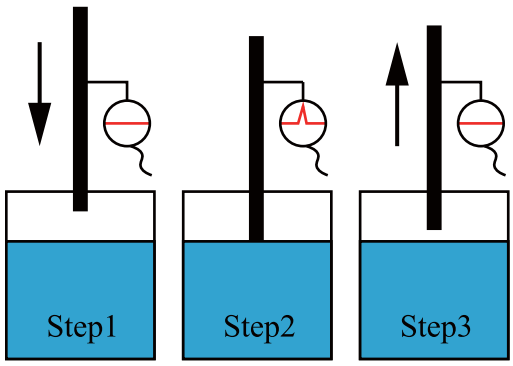

FIG. 5. Schematic views of using current-detection to find the touch point. First, the D/A convertor is fixed to 0 V to continue outputting corrosion voltage. The A/D convertor will monitor the transient signal on each stepper motor's step. Once the transient signal occurs, the position will be recorded. Then, the D/A convertor will be fixed to 5 V to stop outputting corrosion voltage. The stepper motor will lift the tungsten bar up.

Published under license by AIP Publishing

shows, the transient signal in the current-detection region occurs when the tungsten bar touches the electrolyte.

During the experiment, the produced probe was observed to be irregular in shape in certain conditions [Fig. 6(a)]. The bubbles generated during the reaction will float up and affect the meniscus which is related to the formation of the tip's shape. There are three reasons for the emergence of these bubbles. First of all, the prepared sodium hydroxide solution does not stand for enough time. Standing enough time can eliminate these bubbles. Second, the etching reaction [Eq. (1)] will generate hydrogen at the cathode. A partition plate was designed to place between the anode and the cathode [Fig. 2(d)] to prevent the hydrogen from entering the anode. Finally, water electrolysis may react simultaneously at the beginning of electrochemical etching.[16] As is shown in Fig. 6(b), despite the fact that water electrolysis only lasted for a short period of time, the oxygen it generated could not be ignored. A movement of tungsten bar in both vertical and horizontal directions can eliminate this kind of the bubble [Figs. 6(c) and 6(d)]. This process can also be illustrated in the bubble elimination region in Fig. 4(c). Additionally, electrochemical polishing can be carried out to eliminate tungsten bar's oxide layer before tip fabrication [Fig. 4(c)'s Polishment]. The etch workshop's workflow can be seen in Fig. 7.

B. Clean workshop and wrap workshop

Prior to the wrap workshop, the additional clean workshop aims to wipe off crystalline salt (Fig. 8). Although NaOH and Na_2WO_4 are both soluble, surface tension will cause the solution to remain on the tip of the tungsten probe. This workshop comprises of a tank [Fig. 2(c)] and uses oscillation similar to the method in the bubble elimination step mentioned before. The crystalline salt cannot be ignored because it will affect the follow-up procedure. A clean surface is required by wrapping insulating layer and coating platinum film. In addition, crystalline salt composed by NaOH and Na_2WO_4 may cause damage on cell measuring.

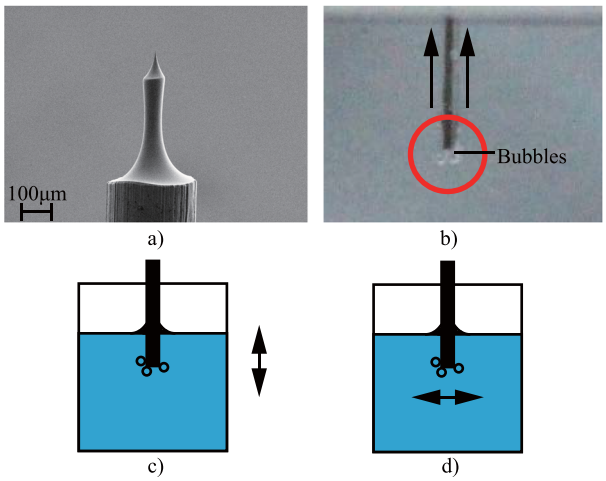

FIG. 6. (a) is one of the probes which are irregular in shape. (b) displayed the bubbles' generation during fabrication. (c) and (d) showed oscillation in both vertical and horizontal directions in order to eliminate bubbles.

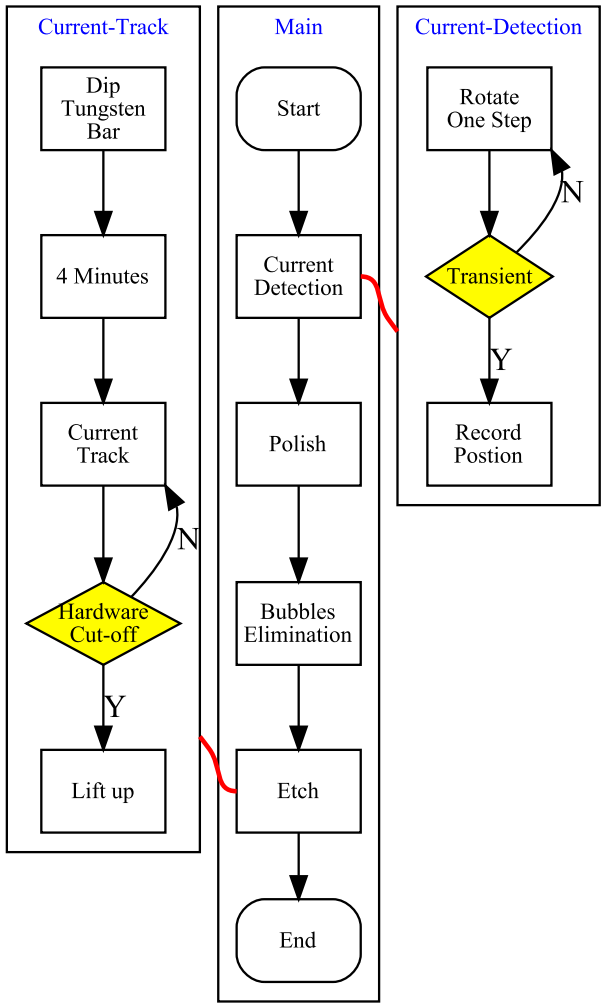

FIG. 7. **Main** is the total workflow of etch workshop fabricating probes. **Current-Track** and **Current-Detection** reveals details of corresponding step in the **Main** flow chart.

Considering biocompatibility and operability, polyurethane (Lubrizol, TT-1085A) is invoked as the W-Pt TC's insulating layer. The wrapping solution was prepared by mixing 30 g polyurethane with 500 ml tetrahydrofuran solution. The wrap workshop consists

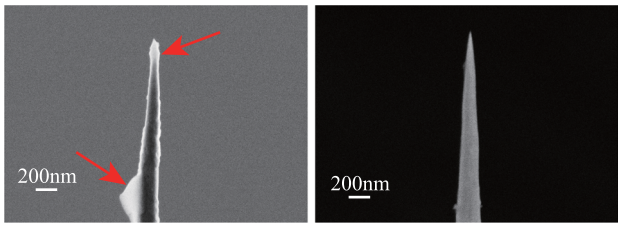

FIG. 8. (a) and (b) are probes fabricated in same control condition: voltage = 6 V, depth = 2 mm, and r_{track} = 0.2. (b) was rinsed after fabricating, while (a) was not.

Published under license by AIP Publishing

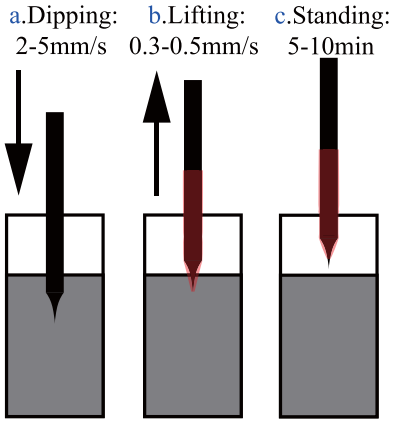

FIG. 9. The one-time workflow of wrapping workshop's involves (a)–(c), respectively, are dipping, lifting and standing.

of eight containers [Fig. 2(b)] with a small diameter to reduce volatilization because tetrahydrofuran is volatile. The wrapping process can be divided into three steps: dipping, lifting, and standing. It is worth nothing that dipping speed requires little attention from researchers. As is shown in Fig. 9(a), the range of 2–5 mm/s makes no difference. However, it is vital to control the speed of lifting. When the probe is lifted, the wrapping solution remains on its surface because of the viscosity. Too high lifting speed means that viscosity plays a leading role during lifting, which causes a thick wrapping layer. What is worse is the solution remaining on the surface will flow gradually. The final insulating layer will be quite thick at the end of probe. Speed at a slow rate makes mobility exercise more effect than viscosity does. The solution remaining on the surface will be extremely thin, thus resulting in bad insulativity. The proper lifting speed range is 0.3–0.5 mm/s [Fig. 9(b)]. The standing time is dependent on lifting speed. High speed leads to a thick wrapping layer, which needs more time to volatilize the tetrahydrofuran. The tip of the probe is exposed due to the break of surface tension [Fig. 9(c)]. The process discussed before can be performed one or multiple times. Based on the engineering experience, 4–5 times is proper.

III. RESULTS AND DISCUSSION

A. Feasibility analysis

As discussed in Sec. II A, U_o changed slowly and was considered to remain unchanged between two acquisitions. For most of the methods, etching voltage, dipping depth, and solution concentration are three main control arguments. As Fig. 4(a) shows, the etching current in the "current-track region" could produce a fitting line with a slope which reveals the U_o's rate of change. The relationship between the slope and three main control arguments is exhibited as blue lines in Fig. 10. For the maximum of slope -6×10^{-2} mA/s, the etching current will change only -6×10^{-5} mA between two acquisitions. In order to improve the output quality, a digital filter can be used in the track signal. As is shown in Fig. 4(a), the Kalman filter was applied in the track signal of the "current-track region." Another factor worth consideration is when to stop the tracking

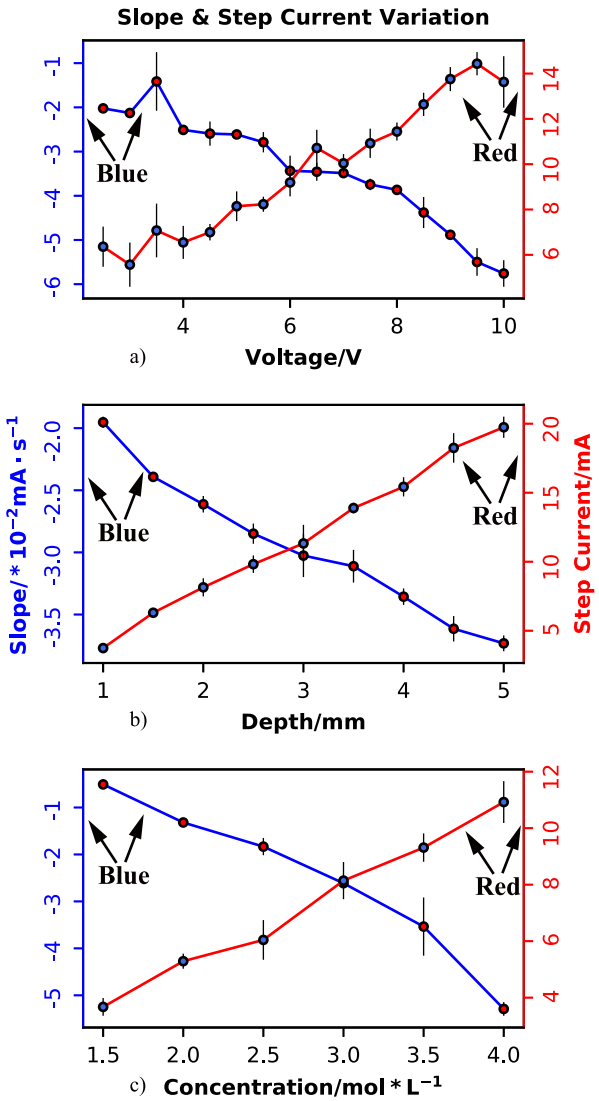

FIG. 10. The relationship of "slope and step current" and three control parameters. (a) used 3 mol/l sodium hydroxide solution and 2 mm dipping-depth. (b) used 6 V etching voltage and 3 mol/l sodium hydroxide solution. (c) used 2 mm dipping-depth and 6 V etching voltage.

signal. When the drop-off happened, the step current was detected as a stop signal. Before this, the range of step current is necessary to be determined. The relationship between step current and three principal control parameters is presented as red lines in Fig. 10. When the acquired voltage is lower than step current in some condition, the current track should be instantly stopped and fixed at 5 V.

Currently, methods of tungsten tip's fabrication mainly include moving or fixing the tungsten bar and using AC (Alternating Current) or DC (Direct Current) during the electrochemical reaction. By the combination of the circuit proposed in the article with a mechanical control system, tips of most shapes can be fabricated by modifying the software only. Figure 11 exhibits different shapes fabricated

Published under license by AIP Publishing

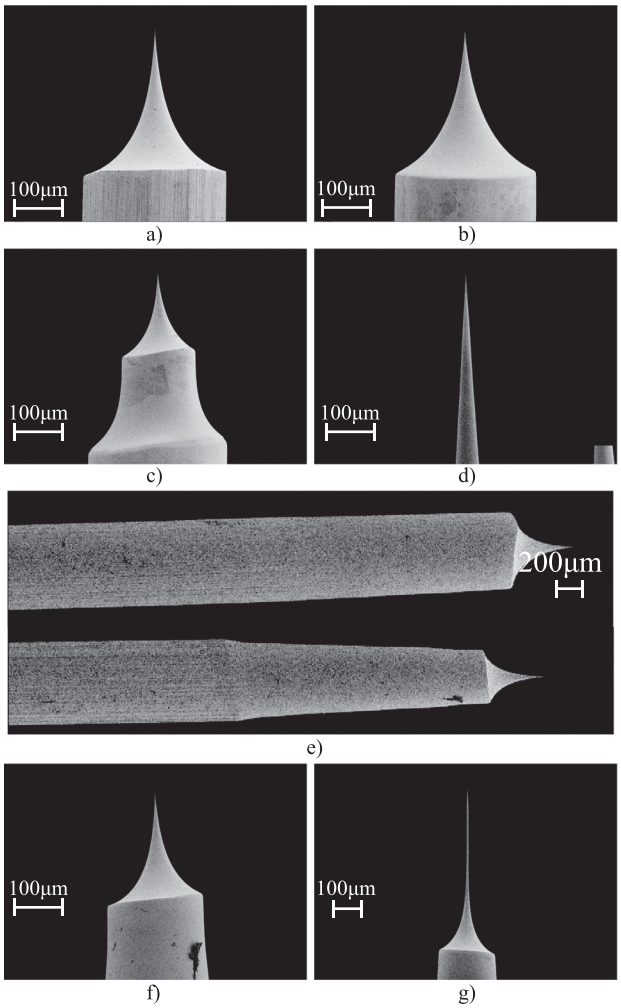

FIG. 11. Tungsten tips with different appearances. (a) U_{etch} = 6 V, L_{depth} = 2 mm, r_{track} = 0.8; (b)–(d) U_{etch} = 10 V, L_{depth} = 2 mm, r_{track} = 0.8; (e)–(g) U_{etch} = 10 V, L_{depth} = 2 mm, r_{track} = 0.95. (a), (b), and (e)'s up tip used the static method; (c) lifted the tungsten bar up during electrochemical reaction; (d) used the oscillation method; (e)'s down tip used the oscillation method for 240 s at the first and static method in the remaining time; (f) was partially enlarged detail of (e)'s down tip; (g) used the oscillation method for 400 s at the first and static method in the remaining time.

by our system. Different voltages make tips with different surface roughness [Figs. 11(a) and 11(b)]. Dynamic electrochemical etching makes the step shape [Fig. 11(c)] and conical shape [Fig. 11(d)]. Combination of static and dynamic electrochemical etching makes the cone-neck [Figs. 11(e) and 11(f)] shape and long-neck shape [Fig. 11(g)]. In conclusion, the current-track method has a good flexibility and generality.

B. Controllable profiles

Profiles of the tungsten tip can be controlled by r_{track}. When the tip starts to form, tension and electrochemical etching work at

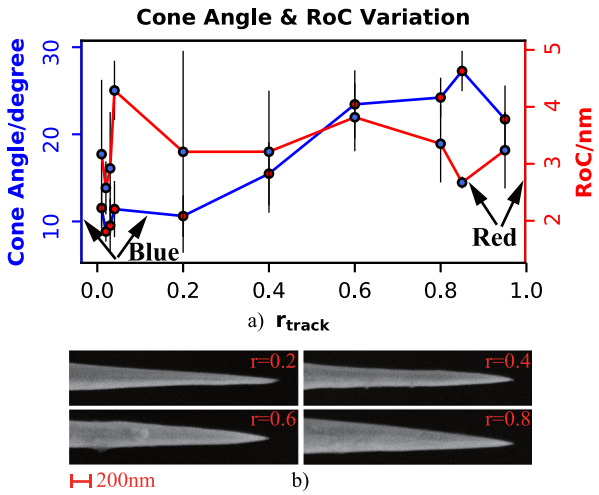

FIG. 12. The relationship of "cone angle and RoC" and r_{track}. (a) and (b) U_{etch} = 6 V, L_{depth} = 2 mm. (a) indicates that the cone angle increases with the growth of r_{track} and RoC keeps from 2 nm to 5 nm; (b) exhibits tips fabricated with different r_{track}.

the same time. Different r_{track} will change the effect time of electrochemical etching by stopping the etching voltage at different points during the formation of the tip, which contributes to different profiles of the tip. As the blue line shows in Fig. 12, the cone angle increases with the growth of r_{track}. The duration of electrochemical etching during the formation of the tip will determine the etched quantity of the final tip. So, the neck of the tip will go upwards. The more etched quantity is, the larger cone angle will be. Moreover, the radius of curvature (RoC) is not affected because the etching

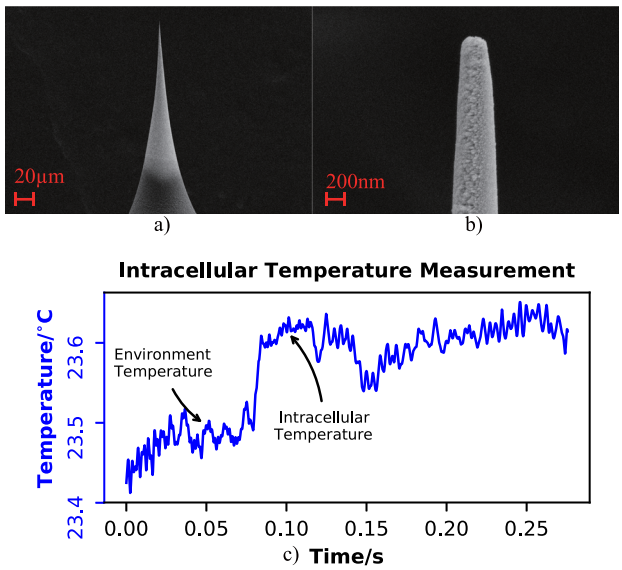

FIG. 13. (a) is the tungsten tip with the insulating layer (W + PU). (b) is the final W-Pt TC sensor (W + PU + Pt). (c) exhibits the temperature change after inserting the sensor into the single cell.

Published under license by AIP Publishing

voltage is stopped before the tension disappears. The continuous current cannot destroy the final tip. Thus, the red line in Fig. 12 reveals the range of RoC is 2 nm–5 nm.

C. Intracellular temperature measurement

The tip with an insulating layer and final W-Pt TC are exhibited in Figs. 13(a) and 13(b). The final W-Pt TC sensor can be used to measure intracellular temperature combined with the optical microscope and micro-nano-manipulator. Figure 13 demonstrates the function of the sensor by inserting the W-Pt TC sensor from outer environment to the single cell's inner. The rising edge reveals the temperature difference between the environment and cell's inner. Apart from several methods of measuring intracellular temperature,[1] cell's temperature has also been verified by multicell temperature measurement.[17,18]

IV. CONCLUSION

Although intracellular temperature measurement has been studied for several years, it is still a new technology to measure the cell's inner temperament by the precise, real-time, and quick-response sensor. W-Pt TC is a kind of nanosensor which is based on electrochemical technology used in fabricating SPM (scanning probe microscopy) tips. One common point between the fabrication of W-Pt TC and SPM tips is applying this kind of nanodevice to microfield. However, the evaluation method of the SPM tips is not suitable for W-Pt TC because it is a brand new sensor fabricated on the basis of totally different theories. What we want to investigate is the relationship between profiles and sensor capability. Nevertheless, there is no classic method that can be generally used since different shapes are made on the basis of various methods among which there exist huge distinctions. Here, a flexible and general control method was proposed to fit all these approaches by combining the software feedback loop with the hardware feedback loop. Last but not least, W-Pt TC has more than one step to be fabricated. The precise control is needed in each step. For the application in biomeasurement area, the cross infection results in huge consumption. The batch fabrication is in urgent demand.

We researched several methods for fabricating SPM tips with different appearances or controllable profiles. The universal control circuit combines an extra software feedback loop with the traditional hardware feedback loop. Using this control strategy, the dipping-depth can be precise. The reaction's on-off can be under control. As a result, the software feedback loop enables us to monitor and control the electrochemical reaction regardless of the use of the AC/DC or dynamic/static method. The parameter r_{track} of the software feedback loop can also be used to control the duration of the electrochemical effect during the tip's formation. This parameter is related to the cone angle, and the controllable range is about 5°–30°. Benefited from the duration control, all the RoCs of tips are less than 5 nm. In conclusion, the structure of three workshops realizes the batch fabrication.

Moreover, one phenomenon that may warrant future research is that in Fig. 14, when r_{track} was less than 6.0×10^{-1}, the formation point of the tip had some possibility to go upwards. This phenomenon never happened when r_{track} was more than 6.0×10^{-1}. In future research, it is valuable to explore the mechanism of this phenomenon.

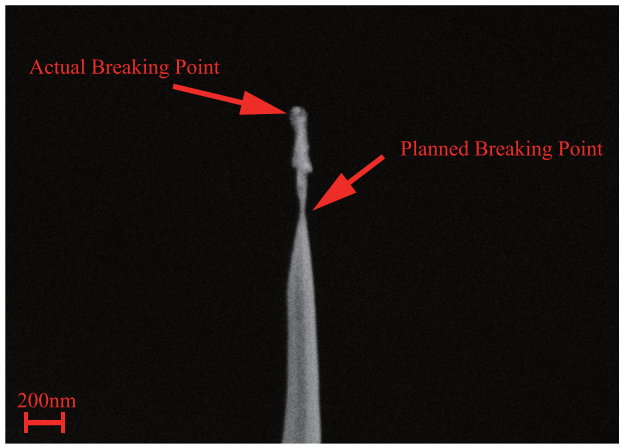

FIG. 14. The figure exhibits the defective tip. The apex of the tip formed at the incorrect point. The phenomenon may occur with r_{track} below 6.0×10^{-1}.

ACKNOWLEDGMENTS

This work was supported by the grants from the National Key Research and Development Program of China (Grant No. 2017YFA0104302) and the National Natural Science Foundation of China (Grant Nos. 61420106012 and 61821002).

REFERENCES

[1] C. D. S. Brites, P. P. Lima, N. J. O. Silva, A. Millán, V. S. Amaral, F. Palacio, and L. D. Carlos, Nanoscale **4**, 4799 (2012).
[2] T. Bai and N. Gu, Small **12**, 4590 (2016).
[3] C. Wang, R. Xu, W. Tian, X. Jiang, Z. Cui, M. Wang, H. Sun, K. Fang, and N. Gu, Cell Res. **21**, 1517 (2011).
[4] J. P. Ibe, P. P. Bey, S. L. Brandow, R. A. Brizzolara, N. A. Burnham, D. P. DiLella, K. P. Lee, C. R. K. Marrian, and R. J. Colton, J. Vac. Sci. Technol., A **8**, 3570 (1990).
[5] B.-F. Ju, Y.-L. Chen, M. Fu, Y. Chen, and Y. Yang, Sens. Actuators, A **155**, 136 (2009).
[6] B.-F. Ju, Y.-L. Chen, and Y. Ge, Rev. Sci. Instrum. **82**, 013707 (2011).
[7] Y. Khan, H. Al-Falih, Y. Zhang, T. K. Ng, and B. S. Ooi, Rev. Sci. Instrum. **83**, 063708 (2012).
[8] Y. Nakamura, Y. Mera, and K. Maeda, Rev. Sci. Instrum. **70**, 3373 (1999).
[9] O. L. Guise, J. W. Ahner, M.-C. Jung, P. C. Goughnour, and J. T. Yates, Nano Lett. **2**, 191 (2002).
[10] D.-I. Kim and H.-S. Ahn, Rev. Sci. Instrum. **73**, 1337 (2002).
[11] W.-T. Chang, I.-S. Hwang, M.-T. Chang, C.-Y. Lin, W.-H. Hsu, and J.-L. Hou, Rev. Sci. Instrum. **83**, 083704 (2012).
[12] P. Kim, J. H. Kim, M. S. Jeong, D.-K. Ko, J. Lee, and S. Jeong, Rev. Sci. Instrum. **77**, 103706 (2006).
[13] T.-H. Duong and H.-C. Kim, Int. J. Precis. Eng. Manuf. **16**, 1053 (2015).
[14] R. Hobara, S. Yoshimoto, S. Hasegawa, and K. Sakamoto, e-J. Surf. Sci. Nanotechnol. **5**, 94 (2007).
[15] J. Wang, T. Nai, W. Tian, and N. Gu, J. Southeast Univ. (Nat. Sci. Ed.) **45**, 673 (2015).
[16] P. I. Ortiz, M. L. Teijelo, and M. C. Giordano, J. Electroanal. Chem. Interfacial Electrochem. **243**, 379 (1988).
[17] C. Li, S. Yan, W. He, S. Yang, J. Sun, and N. Gu, IEEE Trans. Biomed. Eng. **66**, 1898 (2018).
[18] C. Li, J. Sun, Q. Wang, W. Zhang, and N. Gu, IEEE Trans. Biomed. Eng. **66**, 23 (2019).

Published under license by AIP Publishing